Biogeochemistry (2009) 94:271–287
DOI 10.1007/s10533-009-9327-7

The effects of elevated atmospheric CO_2 and nitrogen amendments on subsurface CO_2 production and concentration dynamics in a maturing pine forest

Edoardo Daly · Sari Palmroth · Paul Stoy · Mario Siqueira · A. Christopher Oishi · Jehn-Yih Juang · Ram Oren · Amilcare Porporato · Gabriel G. Katul

Received: 15 January 2008 / Accepted: 17 April 2009 / Published online: 7 May 2009

Abstract Profiles of subsurface soil CO_2 concentration, soil temperature, and soil moisture, and throughfall were measured continuously during the years 2005 and 2006 in 16 locations at the free air CO_2 enrichment facility situated within a temperate loblolly pine (*Pinus taeda* L.) stand. Sampling at these locations followed a 4 by 4 replicated experimental design comprised of two atmospheric CO_2 concentration levels (ambient $[CO_2]^a$, ambient + 200 ppmv, $[CO_2]^e$) and two soil nitrogen (N) deposition levels (ambient, ambient + fertilization at 11.2 g_N m^{-2} $year^{-1}$). The combination of these measurements permitted indirect estimation of belowground CO_2 production and flux profiles in the mineral soil. Adjacent to the soil CO_2 profiles, direct (chamber-based) measurements of CO_2 fluxes from the soil–litter complex were simultaneously conducted using the automated carbon efflux system. Based on the measured soil CO_2 profiles, neither $[CO_2]^e$ nor N fertilization had a statistically significant effect on seasonal soil CO_2, CO_2 production, and effluxes from

E. Daly (✉)
Department of Civil Engineering, Monash University, Building 60, Clayton Campus, Clayton, VIC 3800, Australia
e-mail: edoardo.daly@eng.monash.edu.au

S. Palmroth · M. Siqueira · A. C. Oishi · R. Oren · A. Porporato · G. G. Katul
Nicholas School of the Environment, Duke University, Durham, NC, USA

S. Palmroth
e-mail: sari.palmroth@duke.edu

M. Siqueira
e-mail: mbs4@duke.edu

A. C. Oishi
e-mail: acoishi@duke.edu

R. Oren
e-mail: ramoren@duke.edu

A. Porporato
e-mail: amilcare@duke.edu

G. G. Katul
e-mail: gaby@duke.edu

P. Stoy
School of GeoSciences, Department of Atmospheric and Environmental Science, University of Edinburgh, Edinburgh EH9 3JN, UK
e-mail: paul.stoy@ed.ac.uk

M. Siqueira
Departamento de Engenharia Mecânica, Universidade de Brasília, Brasília, Brazil

J.-Y. Juang
Department of Geography, National Taiwan University, Taipei, Taiwan
e-mail: jjuang@ntu.edu.tw

A. Porporato · G. G. Katul
Department of Civil and Environmental Engineering, Duke University, Durham, NC, USA

the mineral soil over the study period. Soil moisture and temperature had different effects on CO_2 concentration depending on the depth. Variations in CO_2 were mostly explained by soil temperature at deeper soil layers, while water content was an important driver at the surface (within the first 10 cm), where CO_2 pulses were induced by rainfall events. The soil effluxes were equal to the CO_2 production for most of the time, suggesting that the site reached near steady-state conditions. The fluxes estimated from the CO_2 profiles were highly correlated to the direct measurements when the soil was neither very dry nor very wet. This suggests that a better parameterization of the soil CO_2 diffusivity is required for these soil moisture extremes.

Keywords Soil CO_2 dynamics · Climate change · Elevated atmospheric CO_2 · Nitrogen deposition · Fertilization · Loblolly pine

Introduction

Forests contribute to the terrestrial carbon budget by removing CO_2 from the atmosphere through photosynthesis and releasing CO_2 through respiration by vegetation and decomposers in the soil (e.g., Schlesinger 1997; Brady and Weil 2002). Annual soil respiration is a major source of CO_2 into the atmosphere (e.g., Raich and Schlesinger 1992) exceeding the annual anthropogenic fossil fuel emissions by an order of magnitude (Schimel 1995; Schlesinger 1997). Consequently, changes in these fluxes must be considered when assessing the rate at which atmospheric CO_2 concentration increases.

Soil CO_2 efflux has a large potential for amplifying global climate change, yet its role is still debated despite a substantial amount of experimental and theoretical work on the controls of the flux performed in a wide range of ecosystems (Trumbore et al. 1996; Hungate et al. 1997; Cao and Woodward 1998; Cox et al. 2000; Giardina and Ryan 2000; Heath et al. 2005; Palmroth et al. 2005). Many interacting factors affect soil CO_2 efflux by either controlling the production of CO_2 (during root respiration or microbial decomposition) or its transport to the surface. The CO_2 production rate is a function of the amount and activity of the respiring biomass of both roots and soil heterotrophs, with the mass-specific respiration rate (i.e., the activity) depending on temperature and substrate availability (i.e., of photosynthate and decomposable material). The ability of decomposers to access the substrate is, in turn, controlled by additional variables including soil water content. Once produced, the diffusive transport of CO_2 to the surface depends on the CO_2 concentration gradient formed in the soil and the soil CO_2 diffusivity, which, in turn, depends on the air-filled porosity of the soil determined by soil water content (e.g., Chen et al. 2005; Jassal et al. 2005). Thus, although not all the processes that control soil surface CO_2 efflux can be readily quantified in a typical field experiments, many studies have demonstrated that much of the variation in the measured bulk soil CO_2 efflux was attributable to the variation in soil temperature and/or moisture (Davidson et al. 1998, 2006; Palmroth et al. 2005; Gaumont-Guay et al. 2006).

Atmospheric CO_2 concentration and soil nutrient availability also affect carbon cycling in forest ecosystems. Based on a large number of mainly single-factor manipulation experiments (see Hyvonen et al. 2007, for review), increasing atmospheric CO_2 concentration generally increases plant growth through increased canopy carbon uptake, whereas enhanced nutrient availability, especially of nitrogen (N), often causes shifts in carbon partitioning from below to aboveground. Results from forest free air CO_2 enrichment (FACE) experiments suggest that elevated atmospheric CO_2 concentration enhances soil CO_2 efflux (Zak et al. 2000; Butnor et al. 2003; King et al. 2004; Bernhardt et al. 2006; Palmroth et al. 2006). On the other hand, fertilization has been suggested to decrease the total soil CO_2 efflux by suppressing both autotrophic and heterotrophic soil respiration (Makipaa 1995; Bowden et al. 2004; Olsson et al. 2005; Palmroth et al. 2006; Phillips and Fahey 2007). At the Duke Forest FACE prototype experiment in a loblolly pine (*Pinus taeda* L.) plantation, a two factor experiment combined elevated CO_2 treatment (ambient + 200 ppmv) with a nitrogen (N) fertilization treatment (Oren et al. 2001). A shift in carbon partitioning due to fertilization produced a reduction in the total soil CO_2 efflux, even under elevated atmospheric CO_2 (Butnor et al. 2003; Palmroth et al. 2006). However, differences between the CO_2 treatments in soil moisture due to topography and litter buildup (Schäfer et al. 2002) makes it difficult to infer respiratory CO_2 production from efflux, and thus to assess potential interaction effects of elevated CO_2 and N availability on respiration.

Because of the difficulty in performing detailed measurements within the soil, most experiments measure the total soil CO_2 efflux with chambers placed on the litter layer. The observed flux is typically related to soil temperature and moisture measured at some arbitrary depth assumed to be representative of biological activity responsible for respiration. Consequently, the contribution to the soil CO_2 efflux of sources at different soil depths, and the sensitivity of CO_2 production to soil moisture and temperature conditions, which themselves vary vertically, have been rarely investigated and are the subject of this study.

Air-phase soil CO_2 has been measured manually at rather low time resolutions (e.g., weekly or monthly) in a number of ecosystems (Winston et al. 1997; Billings et al. 1998; Rustad and Fernandez 1998; Pumpanen et al. 2003; Bernhardt et al. 2006; Taneva et al. 2006; Hashimoto et al. 2007). However, recent advances in solid-state sensor technologies permit measurements at finer temporal resolution (Hirano et al. 2003; Tang et al. 2003; Jassal et al. 2004, 2005; Chen et al. 2005; Baldocchi et al. 2006). The finer time and depth resolution offered by these datasets permit resolving the interplay between transient environmental factors (e.g., pulsed rainfall) and subsurface CO_2 production and fluxes (e.g., Jassal et al. 2005; Chen et al. 2005).

Here, the simultaneous effects of elevated atmospheric CO_2 and nitrogen amendments on both subsurface CO_2 concentration and production dynamics are quantified at the Duke Forest FACE experiment. In each treatment combination, soil CO_2 production and fluxes at different depths and efflux from the soil to the atmosphere were estimated from the measured profiles of subsurface CO_2, soil moisture and temperature. The estimated CO_2 efflux, representing the fluxes from the mineral soil, was compared at daily and longer time scales to efflux directly measured with chambers positioned on the litter surface.

Methods

Site description

The FACE experiment is located in the Blackwood division of the Duke Forest, Orange County, North Carolina (35°58′N, 79°08′W). Site characteristics are described elsewhere (Oren et al. 1998; Andrews and Schlesinger 2001) and only a brief description is provided here.

The site is located on slightly acidic soils of the Enon series, characterized by relatively low fertility and classified as clayey loam in the upper 30 cm and clay from 30 to 70 cm. Details on the properties of different soil horizons at the site are reported in Oh and Richter (2005). The experiment consists of eight plots (rings), each 30 m in diameter, established in a loblolly pine (*Pinus taeda* L.) plantation. Four treatment plots were fumigated with CO_2 to increase atmospheric concentration by 200 ppmv above ambient concentration levels, while the other four plots were kept at ambient concentration levels (Hendrey et al. 1999). Enrichment commenced in June 1994 in the prototype plot (current plot 7) and was extended to the remaining plots in August 1996. The fumigation was continuous—with the exception of low temperatures and high wind speed conditions—until 2003, when it was reduced to daylight hours only. Litterfall composition and the effect of treatments on its decomposition are discussed by Finzi et al. (2001) and Finzi and Schlesinger (2002).

In 1998, the prototype plot and its reference (current plot 8) were halved, and an impermeable barrier was inserted in the soil up to a depth of 70 cm (more than twice the depth of the fine roots at the site) to conduct a nitrogen by CO_2 manipulation experiment (Oren et al. 2001). The remaining six plots were similarly partitioned in February 2005. One half of each plot (hereafter referred to as a subplot) was fertilized using ammonium-nitrate at a rate of 11.2 g_N m^{-2} $year^{-1}$, appreciably higher than the local addition of N via atmospheric deposition ($\sim$0.8 g_N m^{-2} $year^{-1}$) but typical of N fertilization treatments in loblolly pine plantations.

Accordingly, in terms of belowground activities, four different conditions can be studied: ambient atmospheric $[CO_2]^a$ without fertilizer addition (AU) and with nitrogen fertilizer (AF), and elevated atmospheric $[CO_2]^e$ with ambient conditions (EU) and nitrogen enriched (EF).

Measurements

In each subplot (16 in total), CO_2 concentration (C) in the air phase, soil temperature (T_s), and volumetric soil moisture (θ) were continuously monitored beginning May 2005 at five depths within the upper $\sim$50 cm of soil, thus producing profiles in the zone in which most fine roots are located. The sensors, a total of 240 (80 for each measured variable), were inserted into horizontal holes drilled into the first 50 cm of the vertical face of a pit, which was then carefully back-filled layer-wise to minimize soil disturbance. Given the presence of large roots and rocks, the precise sensor depths and position with respect to the other sensors varied slightly from plot to plot.

Soil CO_2 concentration time series were measured with solid-state infrared CO_2 transmitters (GMT 221 model, Vaisala, Finland; e.g., Tang et al. 2003; Jassal et al. 2005; Chen et al. 2005), with a measurement range from 0 to 50,000 ppmv (10,000 ppmv = 1% CO_2 = 10 mmol mol^{-1}) and accuracy of ±200 ppmv + 2% of the reading. The sensors were tested with reference gases at 0 and 10,000 ppmv. A laboratory test conducted with sand showed that continual operation of the CO_2 sensors increases the temperature around the head of the sensor by up to 2°C, as has also been reported by Jassal et al. (2004). Although such heating has the potential to increase soil respiration rates in the immediate proximity of the probe (Baldocchi et al. 2006), it helps prevent water from condensing inside the sensor element, thus reducing the possibility for probe malfunctioning.

Soil temperature profiles were constructed from thermocouple measurements (105T-L16, Campbell Scientific Inc.) vertically installed about 30–40 cm apart from the CO_2 sensors at the same soil depth. Volumetric soil water content was measured with Theta Probes (model ML2x, Delta-T Devices, Cambridge, UK, distributed by Dynamax Inc., Houston, TX, USA). Given the high rock content and the fact that the soil is mainly composed of clay, some vertical profiles of soil water content exhibited complex vertical patterns, possibly due to localized interferences from nearby rocks, or local air pockets.

Throughfall (P_t) was also measured with tipping bucket gages (TE525, Campbell Scientific Inc.) in each of the eight plots near the place where the two vertical sensor arrays were installed. All sensors were interrogated every 30 s and 30 min averages (sums for P_t) were recorded.

From July 2005, forest floor CO_2 efflux (F_m) time series were also measured about 30 cm far away from the vertical arrays using the Automated Carbon Efflux System (ACES, U.S. Patent 6,692,970) developed at the USDA Forest Service, Southern Research Station Laboratory in Research Triangle Park, NC and described in Butnor et al. (2003) and Butnor and Johnsen (2004).

Data processing

The concentration readings of the CO_2 sensors were corrected to account for temperatures different from the reference temperature, 25°C. Such a correction was computed from the empirical relationship provided by the manufacturer (personal communication, Vaisala Inc.)

$$C = C_m - C_T, \tag{1}$$

where the corrected CO_2 concentration, C (in ppmv), is evaluated from the measured concentration, C_m (in % CO_2), by subtracting the term

$$C_T = 14000(K - K^2)\frac{25 - T_s}{25}, \tag{2}$$

with $K = A_3C_m^3 + A_2C_m^2 + A_1C_m + A_0$, $A_3 = 7.9 \times 10^{-6}$, $A_2 = -10^{-3}$, $A_1 = 6.7 \times 10^{-2}$, and $A_0 = 8.4 \times 10^{-3}$. The correction term C_T is of the same order of magnitude as the instrument error during most of the measurement period, becoming only relevant during winter. Hence, the correction does not significantly affect the main period of our analyses—the growing season.

Statistical analyses

The treatment effects on the annual soil CO_2 concentration and respiration were evaluated using a split-plot ANOVA analysis (Steel et al. 1997). The atmospheric CO_2 enrichment, randomly assigned to four of the plots, was considered as the main factor with N fertilization assigned at random to one half of each plot (i.e., subplot) as a nested factor. In the following analyses, missing values are replaced by the average of the other subplots subjected to the same combination of treatments.

CO_2 fluxes and production

The measured soil CO_2 concentration, temperature, and soil moisture time series can be used to compute CO_2 fluxes and CO_2 production profiles at each subplot by using the continuity equation. Given the large CO_2 concentration vertical gradients, horizontal transfer can be neglected. Accordingly, the continuity equation for CO_2 concentration, both in the gas (C) and dissolved phase (C_w), can be modeled as (Simunek and Suarez 1993; Fang and Moncrieff 1999)

$$\frac{\partial}{\partial t}(f_a C + \theta C_w) = -\frac{\partial}{\partial z}(F + q_w C_w) - E C_w + S, \quad (3)$$

where t is time, z is the vertical direction (positive upward), f_a is the air-filled porosity, F describes the flux by diffusion in the gas phase, q_w is the soil water flux, E is the water uptake by plant roots, and S is a source/sink term accounting for biological production (i.e., root and microbial respiration) and other possible mechanisms of CO_2 movements, such as air fluxes. Flux caused by dispersion in the dissolved phase is neglected because it is 10^{-4} of that due to diffusion in the gas phase (Glinski and Stepniewski 1985; Simunek and Suarez 1993; Fang and Moncrieff 1999). In one-dimensional approaches, the modeling of air-displacement is difficult and arbitrary (Simunek and Suarez 1993) and thus was not included in this analysis. However, the contribution of this term is not expected to be significant except during strong rainfall events (as we show later).

Dissolved CO_2 can be related to the CO_2 concentration in the gas phase by assuming that the total dissolved CO_2 is present as carbonic acid, H_2CO_3 (e.g., Fang and Moncrieff 1999), and that the equilibrium between CO_2 and H_2CO_3 is sufficiently fast to permit the application of Henry's law (Glinski and Stepniewski 1985; Simunek and Suarez 1993; Flechard et al. 2007). Accordingly, the CO_2 concentration in the liquid phase becomes

$$C_w = \alpha_H R T_s C, \quad (4)$$

where α_H is Henry's law constant, the value of which was extrapolated from the data in Glinski and Stepniewski (1985), and R is the universal gas constant (8.314 kg m^2 s^{-2} K^{-1} mol^{-1}). Given the acidity of the soil in this forest (pH $\cong$ 5–6, Oh and Richter 2005), dissociated (bicarbonate and carbonate) forms of CO_2 in water are at least one order of magnitude lower than H_2CO_3 (Flechard et al. 2007) and are thus neglected.

The gas-phase fluxes are assumed to follow Fick's law (e.g., Patwardhan et al. 1988; Simunek and Suarez 1993; Chen et al. 2005), given by

$$F = -D(\theta, T_s)\frac{\partial C}{\partial z}, \quad (5)$$

where D is the diffusivity of CO_2 in the soil gas phase. The adoption of the Fick's law appears adequate for CO_2, while Stefan–Maxwell equations should be applied for a multi-component diffusion process (see Thorstenson and Pollock 1989; Fang and Moncrieff 1999; Freijer and Leffelaar (1996) for a comparison of the two formulations).

The diffusivity coefficient in Eq. 5 is modeled using the classical tortuosity formulation derived by Millington (1959) and Millington and Quirk (1961)

$$D = D_a\left(\frac{T_s}{293}\right)^{1.75}\frac{f_a^{\alpha}}{n^2}, \quad (6)$$

with $D_a = 15.7$ mm^2 s^{-1} being the molecular diffusion coefficient for CO_2 in free air at 293 K (e.g., Campbell and Norman 1998) and a = 10/3 a semi-empirical coefficient. The form of the diffusivity in Eq. 6 with a = 10/3 was earlier employed at the same site by Suwa et al. (2004), who reported good agreement between chamber measured and modeled F near the surface. Soil porosity in Eq. 6 is evaluated as $n = 1 - \rho_b/\rho_p$, with ρ_b and ρ_p being the bulk density and particle density for the mineral soil, respectively. Bulk densities were estimated by fitting a second order polynomial to the values for soil of the Enon Series reported in Oh and Richter (2005), while typical ρ_p of 2.65 g cm^{-3} was used (e.g., Brady and Weil 2002).

The transport of dissolved CO_2 due to soil water fluxes and transpiration, $q_w C_w$ and EC_w, was neglected because they are commonly much lower than the other terms in Eq. 3. The highest water fluxes occur during and following rainfall events. If we assume that under these conditions, the top-soil is entirely saturated, the fluxes become of the same order of magnitude as the soil hydraulic conductivity at saturation, which has been estimated to be about 0.08 $m^3_{H_2O}\, m^{-2}_{soil}$ day^{-1} (Oren et al. 1998; Suwa et al. 2004). In the upper soil layers ($\sim$5–6 cm) the largest CO_2 concentrations are about 10^4 $\mu mol_{CO_2}\, mol^{-1}_{air}$, which correspond to about 4×10^5 $\mu mol_{CO_2}\, m^{-3}_{H_2O}$ of dissolved CO_2 concentrations (see Eq. 4 where $\alpha_H R T_s \cong 1\ m^3_{air}\, m^{-3}_{H_2O}$; e.g., Glinski and Stepniewski 1985). Accordingly, the product $q_w C_w$ is approximately 0.4 $\mu mol_{CO_2}\, m^{-2}_{soil}$ s^{-1}, an order of magnitude lower than F at the soil surface, F_s. Considering that the hydraulic conductivity diminishes dramatically as soil moisture decreases, the expected water fluxes are at least an order of magnitude lower than those estimated at saturation, and therefore $q_w C_w$ can be usually neglected.

With respect to the term EC_w, transpiration rates on the order of $2 \times 10^{-3}\ m^3_{H_2O}\ m^{-2}_{soil}\ s^{-1}$ have been reported using sapflow measurements (Oren and Pataki 2001; Phillips and Oren 2001). Assuming for simplicity that the root profile is uniformly distributed over the first 40 cm of soil, E is about $6 \times 10^{-8}\ m^3_{H_2O}\ m^{-3}_{soil}\ s^{-1}$. The product EC_w is thus about $2 \times 10^{-2}\ \mu mol_{CO_2}\ m^{-3}\ s^{-1}$, which, as will be demonstrated later, is two orders of magnitude lower than the common values of the terms S and the divergence of the fluxes, $-\partial F/\partial z$.

Based on the analyses above, Eq. 3 can be rewritten to provide estimates of the production (S)

$$\frac{\partial}{\partial t}[(f_a + \theta \alpha_H R T_s)C] - \frac{\partial}{\partial z}\left(D(\theta, T_s)\frac{\partial C}{\partial z}\right) = S, \qquad (7)$$

where the terms on the left hand side can be estimated using the time series of C, θ, and T_s collected at different depths (e.g., Tang et al. 2003; Suwa et al. 2004; Chen et al. 2005; Jassal et al. 2005). The estimate of the fluxes, $-D\partial C/\partial z$, at the surface, assumed equal to respiration from the mineral soil, F_s, is calculated by assuming constant concentration at the soil surface equal to that in atmosphere, which is either 380 or 580 ppm depending on the treatment.

Because depth and time gradients are required in the calculation of S, data conditioning is necessary. In the time domain, the series were smoothed with a Savitzky–Golay filter, which preserves the height and the width of the peaks in the series (Savitzky and Golay 1964; Chen et al. 2005). Such a filter adopts a moving average procedure, according to which the smoothed values, X_k, are evaluated using

$$X_k = \frac{\left(\sum_{i=-m}^{i=+m} B_i x_{k+i}\right)}{N}, \qquad (8)$$

where x_{k+i} are sequential events from the original data series, B_i are convoluting integers depending on the number chosen for m (here 8) and on the degree of the polynomial adopted to interpolate the points x_{k+i}, and N is a normalizing factor. We employed B_i and N for a cubic polynomial (e.g., Savitzky and Golay 1964; Chen et al. 2005).

Moreover, the vertical CO_2 concentration profiles were fitted as a quadratic function of depth (e.g., Takle et al. 2004; Jassal et al. 2005). We also experimented with other interpolation schemes and found the following: (a) a linear interpolation of the data leads to unrealistic fluxes and mostly negative values of S indicating net CO_2 uptake, an unlikely case in the soil pores; (b) a third order polynomial resulted in an overestimation of the fluxes and unrealistically small concentration values at the surface; and (c) other higher-order interpolation schemes, such as cubic spline, also generated source profiles with too many artificial oscillations.

Results and discussion

The effects of the two treatments, elevated atmospheric $[CO_2]^e$ and N fertilization, on subsurface CO_2 and production are evaluated here. The subsurface CO_2 profiles during the years 2005 and 2006 are presented first, followed by estimates of CO_2 production and fluxes. The estimates of production and fluxes are restricted to 2006 because, unlike the discontinuous data in 2005, there were few short gaps in the data during this year. In addition, measurements of the soil fluxes with the ACES chambers, used in evaluation of flux estimates, were available only since the latter part of 2005 growing season.

Subsurface CO_2 concentrations

Effects of the treatments

The mean values of C and soil temperature (T_s) over the first 30 cm and the total throughfall, P_t, during the two monitored growing seasons are reported in Table 1. The growing season is defined as the period of time during the year in which the soil temperature in the first 30 cm remains consistently higher than 15°C. Thus, the length of the season varies slightly among the plots and between the 2 years. The differences in throughfall among the plots may be due to spatial variability in plant area density (Oren et al. 2006), which also causes different solar radiation interception. Despite such spatial variability, soil temperatures were similar in all plots over the entire period of observation (data not shown).

Table 1 Time averages of soil CO_2 concentration (C) and soil temperature (T_s) vertically averaged over 30 cm depth (vertical averaging indicated by < >) and total throughfall (P_t) during the 2005 and 2006 growing seasons (column DOY reports the period during which soil temperatures are consistently higher than 15°C) for each treatment

	FACE ring	2005				2006			
		$\langle C \rangle$ (mmol mol^{-1})	$\langle T_s \rangle$ (°C)	P_t (mm)	DOY	$\langle C \rangle$ (mmol mol^{-1})	$\langle T_s \rangle$ (°C)	P_t (mm)	DOY
AU	1	6.97 (1.85)	21.42 (3.25)	241.5	130–310	7.84 (2.28)	20.45 (3.47)	338.9	147–298
	5	8.70 (3.00)	22.53 (3.61)	241.7	154–322	9.99 (2.15)	22.44 (2.86)	405.5	147–298
	6	10.74 (4.22)	21.95 (3.78)	328.0	133–322	14.08 (4.50)	21.05 (3.91)	464.5	145–320
	8	11.78 (5.38)	22.21 (3.63)	240.3	143–323	15.79 (6.11)	21.45 (3.70)	504.7	144–321
		9.94 (3.37)				**12.4 (3.31)**			
AF	1	7.22 (2.30)	21.38 (3.44)	241.5	130–310	8.43 (3.07)	20.36 (3.69)	338.9	147–298
	5	9.80 (2.65)	22.07 (3.64)	241.7	154–322	10.45 (1.70)	22.12 (2.88)	405.5	147–298
	6	8.12 (2.75)	22.13 (3.47)	328.0	133–322	9.32 (2.47)	21.19 (3.44)	464.5	145–320
	8	7.26 (4.12)	22.25 (3.87)	240.3	143–323	8.66 (3.21)	21.38 (4.00)	504.7	144–321
		8.39 (2.75)				**9.58 (2.41)**			
EU	2	12.16 (3.50)	22.00 (3.88)	256.0	136–322	15.32 (3.65)	22.10 (2.92)	379.0	147–298
	3	7.24 (2.76)	21.02 (3.47)	207.3	155–322	11.59 (4.26)	21.42 (3.74)	480.4	146–321
	4	9.84 (3.77)	22.41 (2.90)	193.8	150–310	–	20.86 (3.50)	373.4	146–321
	7	7.61 (3.25)	21.88 (3.51)	215.4	150–323	7.34 (2.59)	21.04 (3.61)	492.3	144–321
		9.57 (3.03)				**11.68 (3.42)**			
EF	2	12.09 (3.16)	21.48 (3.43)	256.0	136–322	14.50 (3.59)	21.79 (2.58)	379.0	147–298
	3	8.41 (2.53)	21.55 (3.31)	207.3	155–322	9.55 (2.49)	21.57 (3.61)	480.4	146–321
	4	7.04 (2.18)	22.56 (3.10)	193.8	150–310	–	20.86 (3.72)	373.4	146–321
	7	6.24 (1.92)	21.70 (3.47)	215.4	150–323	7.46 (1.99)	20.79 (3.54)	492.3	144–321
		8.76 (2.18)				**10.71 (2.38)**			

Standard deviations are reported between parentheses. Treatment averages and standard deviations of C are reported in bold

AU ambient unfertilized, *AF* ambient fertilized, *EU* enriched unfertilized, *EF* enriched fertilized

A split-plot ANOVA (Steel et al. 1997) showed that the growing-season averages of C were not significantly affected by the treatments or their interaction. C was $\sim$30% higher in 2006 (Fig. 1) because of the higher θ. The averages were primarily controlled by local conditions, as suggested by the consistent differences among plots in both years.

This result is in agreement with that obtained by Taneva et al. (2006) and Bernhardt et al. (2006), who found no statistically significant impact of enriched atmospheric CO_2 on soil C sampled at the same site at depths from 0.15 up to 2 m during the years 1996–2004. On the other hand, it contrasts the findings of Suwa et al. (2004) that subsurface CO_2 concentration was often greater in elevated CO_2 FACE rings from 1997 to 2000 (from 0.15 m up to 2 m, sampled monthly). However, in this regard we note that Suwa et al. (2004) found that the stimulating effect of enriched atmospheric $[CO_2]^e$ in the first 30 cm decreased in time from 1997, when the experiment started, to 2004. According to this observed decreasing trend, the enhanced annual mean soil CO_2 concentration next to the surface related to the CO_2 fumigation almost disappeared in 2004. This is consistent with our observation in 2005 and 2006.

C dynamics at different depths and time-scales

Figure 2 shows examples of measured time series from the fertilized subplot of one of the ambient plots (plot 1, AF, see Table 1). These series are representative of trends at all subplots. While C often increases with increasing depth, shallower depths can occasionally reach concentration levels higher than those at the deeper soil layers (Fig. 2a). Such conditions are generally limited to short periods after

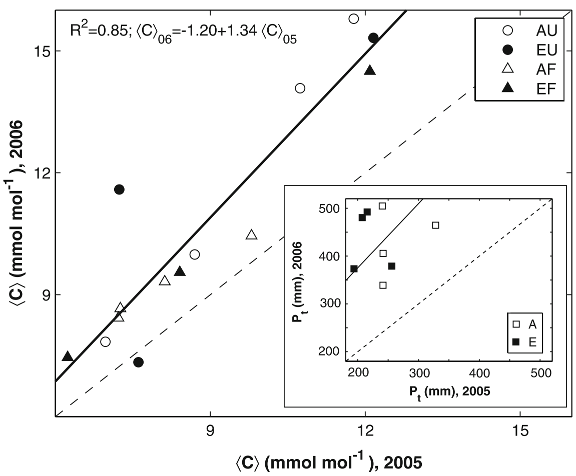

Fig. 1 ⟨*C*⟩ (growing season average of air-phase soil CO_2 concentrations averaged over 30 cm of depth) during 2005 against 2006 (see Table 1). The intercept of the regression line is not significantly different from 0 ($P > 0.1$). *Circle* and *triangle* refer to unfertilized and fertilized conditions, respectively, and *open* and *filled* symbols to ambient and elevated atmospheric [CO_2], respectively. The *inset* shows the relationships between total throughfall during the growing seasons 2005 and 2006

rainfall events. In fact, rainfall events are commonly followed by *C* pulses (Xu et al. 2004; Jassal et al. 2005; Palmroth et al. 2005; Daly et al. 2008), which occur almost immediately in the shallow subsurface zone, and are often delayed by up to 1 h at deeper soil layers, likely reflecting the reduction in CO_2 diffusivity with the propagation of the water infiltration front (Chen et al. 2005; Jassal et al. 2005).

Apart from fluctuations related to rainfall events, there is a weak seasonal oscillation in *C* at shallow depths (Fig. 2a), as was observed in other field studies (e.g., Hirano et al. 2003; Pumpanen et al. 2003; Jassal et al. 2005). In contrast, a seasonal cycle is evident at deeper layers (Fig. 2a) in phase with that of soil temperature (Fig. 2c).

C also shows cyclic behavior at the daily scale. Figure 3 presents a comparison between daily oscillations of T_s and *C* typical of different seasons in 2005 and 2006 at different depths. The periods during which soil temperature averaged over 30 cm increases from 10 to 20°C and decreases from 20 to 10°C are defined as 'spring' and 'fall', respectively, while the periods when temperature is commonly higher than 20°C or lower than 10°C are defined as 'summer' and 'winter', respectively. The curves in Fig. 3 are obtained by (1) subtracting from each rain-free day the midnight-to-midnight daily trend and the daily average of T_s and *C*, respectively; (2) grouping the days into four different seasons, and then (3) constructing the ensemble averages over all the selected days. The midnight-to-midnight daily trend is assumed linear. Maxima and minima of daily averaged temperatures show an approximate 2 h delay at 25 cm compared to T_s nearest to the soil surface during the entire year (Fig. 3a). As expected,

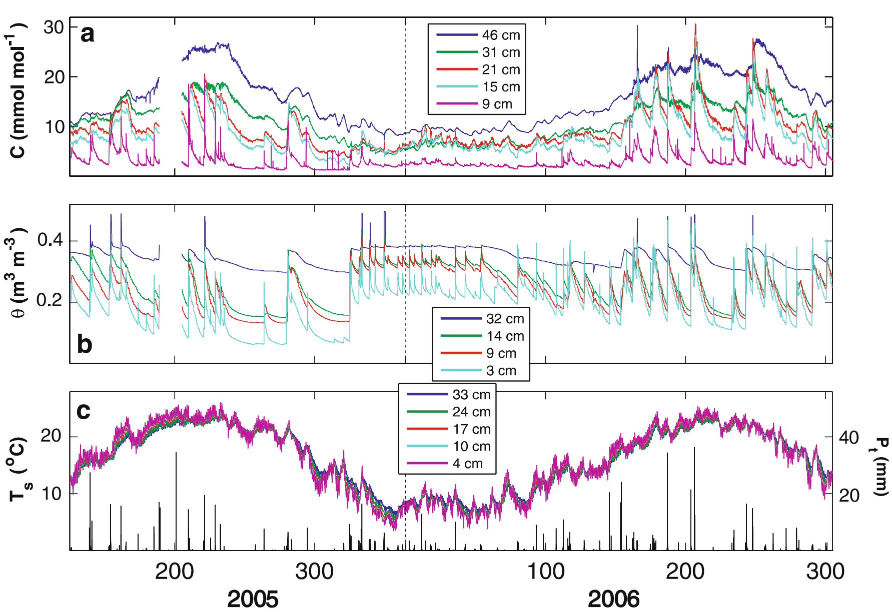

Fig. 2 Examples of time series of **a** measured soil CO_2 concentration (*C*), **b** soil volumetric water content (*θ*), **c** soil temperature (T_s), and throughfall (P_t) for the fertilized plot in plot 1 (AF1) of Table 1. One of the time series of soil moisture is not reported because of sensor malfunction

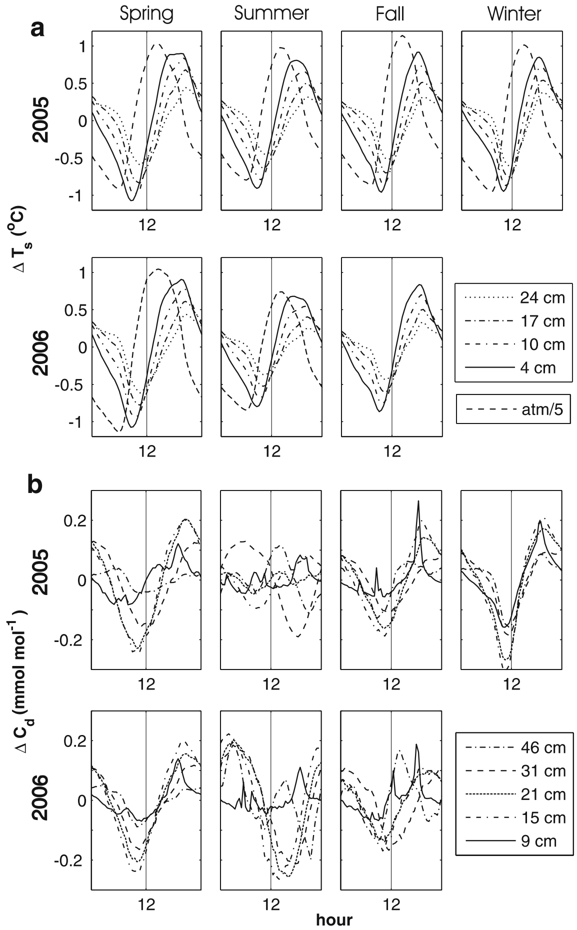

Fig. 3 Ensemble-averaged daily oscillations in T_s and C for different seasons in 2005 and 2006 in plot AF1 (see Fig. 4). Atmospheric temperature (divided by 5) is also reported in **a**

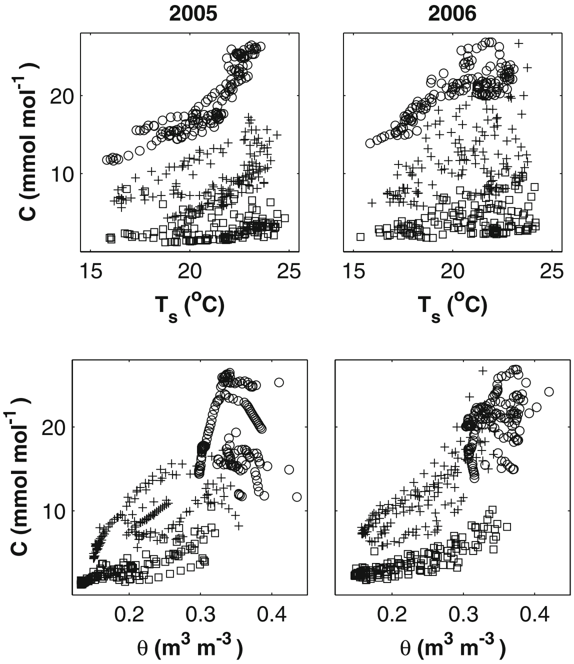

Fig. 4 Examples (plot AF1 of Table 1) of the relationships between daily soil temperature (T_s), daily soil moisture (θ), and CO_2 concentration (C) at three different depths: 46 cm (*circle*), 15 cm (+), and 9 cm (*square*) during the years 2005 and 2006

the amplitude of the oscillations is more pronounced near the surface.

In contrast to soil temperature, daily C oscillations vary with depth and season (Fig. 3b). A daily cycle is not evident close to the surface, where C is strongly impacted by soil water and C fluxes next to the soil surface. Moving downward within the soil column, the oscillations in C gradually shift from being in phase with temperature during most of the year to being out of phase from spring to fall. These oscillations return to be in-phase with temperature during winter, possibly because of the low microbial and root activities (see Fig. 3b).

Although daily cycles of C and T_s are less related at deeper soil layers, the daily mean values of C at these depths have clear relationships with T_s. As shown in Fig. 4, variations in C are related to soil temperature changes at 32 cm. Moving upward to 9 cm depth, this relation becomes less evident and large variations in C can be seen for the same values of temperature. In contrast, daily C is less related to soil moisture at the deeper layers, where C shows large variations, despite low variability in θ (Fig. 4).

In summary, the relationships between C and T_s and θ vary depending on the timescale and depth. Both C and T_s have daily oscillation at all depths, while θ monotonically decreases in time between rain events at each depth, showing little seasonal fluctuations at the deeper soil layers. At shallow depths, daily average C is related to θ. At deeper soil layers (below $\sim$25 cm), C and T_s show strong seasonal cycles and the variation in C is weakly related to variations in θ. This might suggest that CO_2 concentration is affected more by soil moisture near the surface, where soil water pulses following rainfall events introduce a strong perturbation, while at deeper soil layers, where soil moisture does not significantly vary, CO_2 variations can be mainly related to temperature.

Rainfall-induced variation in C near the soil surface

The relationships between C and θ near the surface (i.e., less than 10 cm) are reflected in surface fluxes and their intermittent behavior with rainfall (e.g., Daly et al. 2008). At the daily time scale, when C and total infiltrating water are considered, consistent linear trends among different plots emerge.

Because daily throughfall ($P_{t,d}$) and the consequent increase in soil surface θ are linearly related (not shown), we analyze and discuss C directly with respect to $P_{t,d}$. We define a rainfall-induced C pulse (ΔC) at the daily timescale as the difference between the daily [CO_2] measured the day after a rainfall event and that measured the day before the same rain event. The relationship between the magnitudes of C pulses and $P_{t,d}$ tends to be quasi-linear with constant slope for the 2 year study period and in almost all the plots (Fig. 5; Table 2). The differences among the slopes of the lines in different plots are likely to be related to local soil-vegetation conditions and partly to the uncertainty in determining the exact vertical position of the sensors. There is uncertainty in determining the location of the transition zone between litter and soil, and integrating volumes of the soil moisture and C sensors themselves. The responses of ring 7 and 8 in 2005 were very different from that in 2006. These differences are probably due to similar local soil properties (the two rings are very close to each other). At the daily timescale, ΔC appears independent of the various values of daily θ prior to rainfall events. This suggests that ΔC is due to reductions in gas-phase diffusivity rather than to a sudden increase in respiration following the rainfall events (e.g., Lee et al. 2004; Chen et al. 2005). The two treatments did not affect the relationships in Fig. 5, as was supported by the split-plot ANOVA analysis (lowest $P = 0.05$).

CO_2 production and fluxes

Next, the subsurface CO_2 concentration data along with the θ, and T_s profile measurements are used to estimate subsurface CO_2 production (S) and fluxes (F) during 2006. For illustration, we report in detail the analyses for two subplots of one plot (AU1 and AF1).

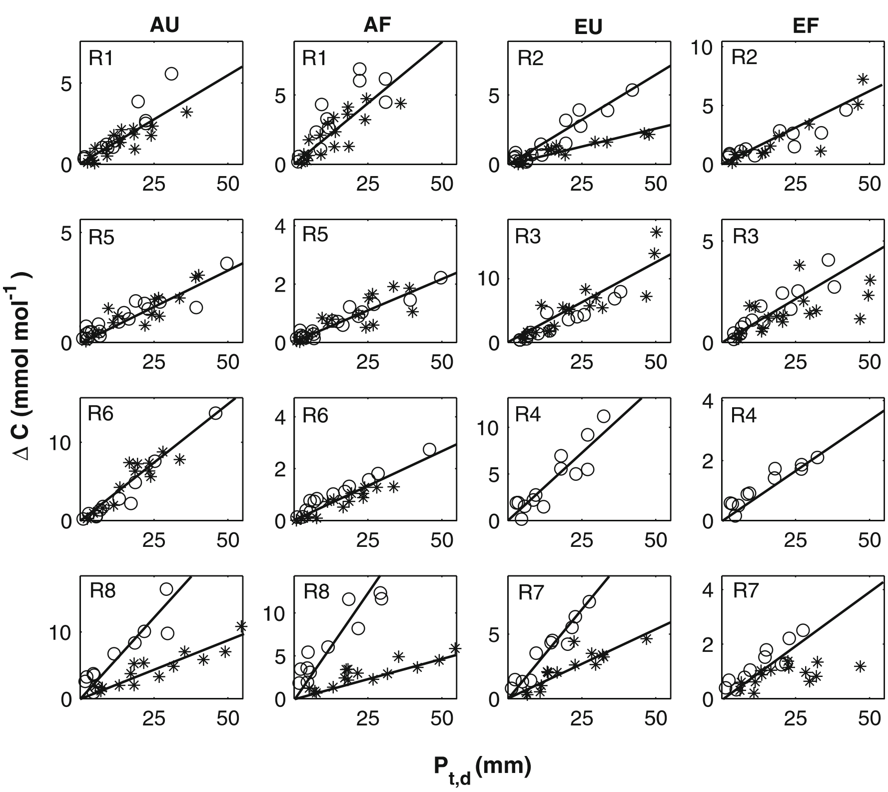

Fig. 5 Relationships between daily throughfall ($P_{t,d}$) and CO_2 concentration pulses (ΔC) in all the FACE rings (R1,…, R8) during 2005 (*circle*) and 2006 (*star*). The regression slopes and coefficients of determination are reported in Table 3

Table 2 Regression slopes (mmol CO_2 mol^{-1} mm^{-1} H_2O) and coefficients of determination, r^2, for the regression lines in Fig. 5

FACE ring		AU		AF		FACE ring		EU		EF	
		Slope	r^2	Ring	r^2			Slope	r^2	Slope	r^2
1	2005	0.15	0.86	0.22	0.66	2	2005	0.12	0.89	0.10	0.76
	2006	0.09	0.76	0.15	0.63		2006	0.05	0.86	0.12	0.85
		0.11	0.71	0.18	0.60			–	–	0.11	0.83
5	2005	0.07	0.80	0.04	0.92	3	2005	0.19	0.90	0.09	0.85
	2006	0.07	0.79	0.04	0.64		2006	0.25	0.78	–	–
		0.07	0.79	0.04	0.78			0.23	0.79	–	–
6	2005	0.27	0.93	0.06	0.92	4	2005	0.29	0.82	0.72	0.83
	2006	0.29	0.81	0.04	0.87		2006	0.20	0.59	–	–
		0.28	0.89	0.05	0.81			0.23	0.63	–	–
8	2005	0.46	0.82	0.45	0.76	7	2005	0.27	0.91	0.09	.74
	2006	0.17	0.80	0.11	0.72		2006	0.11	0.76	–	–
		–	–	–	–			–	–	–	–

Data are not available in one plot (plot 4, fertilized) for 2006. Data from plots 7 and 8 and plot 2 unfertilized had different behavior than the other rings during the measurement period. Data from plots 7 and 3 in the fertilized treatment could not be fitted with a linear relationship in 2006

Effect of the treatments

Table 3 reports the average amount of carbon respired per day in the plots using Eqs. 5 and 6 with $\alpha = 10/3$. As with $\langle C \rangle$, our spatial resolution could be insufficient to capture the spatial variability and, thus, the treatment effects. Such effects were captured in other studies (Butnor et al. 2003; Palmroth et al. 2006) in the case of ring 7 and 8 with a higher spatial resolution.

Soil CO_2 storage

The estimation of the first term in Eq. 7 shows that the subsurface CO_2 storage usually varies slowly, with values that are commonly largely lower than the flux divergence (i.e., the second of Eq. 7), and thus also smaller than the C production, S (Fig. 6). Changes in CO_2 storage in both air and water phases are usually low during the entire year except during rainfall events, when large oscillations occur (Fig. 6). When water infiltrates the soil, air-phase ($f_a C$) and dissolved CO_2 (θC_w) have opposite dynamics: $f_a C$ decreases because of the reduction of air-filled porosity, while the soil contains more dissolved CO_2 because of higher volumetric soil moisture. The changes of f_a and θ during and right after rainfall events appear more important than the increase of C and the decrease of C_w in determining the variations of total CO_2 storage. The variations are lower at the

Table 3 Averaged daily carbon (g_C m^{-2} day^{-1}) respired in the year 2006 in the different plots as estimated from the vertical arrays

FACE ring	2006		FACE ring	2006	
	AU	AF		EU	EF
1	2.85 (2.25)	2.61 (1.89)	2	4.54 (4.05)	–
5	–	2.74 (1.69)	3	3.55 (2.02)	4.66 (2.73)
6	3.83 (2.69)	4.34 (2.63)	4	3.42 (2.48)	4.65 (2.51)
8	5.42 (3.99)	1.64 (1.18)	7	2.1 (1.30)	3.6 (2.20)
	4.04 (2.76)	**2.83 (1.74)**		**3.41 (2.34)**	**4.31 (2.41)**

The averages are calculated over 365 days. The vertical arrays in the fertilized plot in ring 2 and in the unfertilized plot in ring 5 are not reliable because of external disturbances. The fluxes in ring 4 during 2006 have been evaluated using only the sensor near the top, since most of the other sensors did not work properly during this year. Standard deviations are reported between parentheses. Treatment averages and standard deviations are in bold

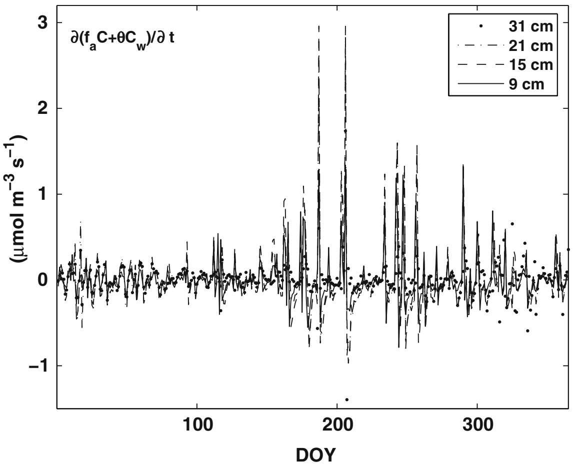

Fig. 6 Rate of change of daily CO_2 storage in both aqueous and gas phase at different soil depths in the plot AF1 during 2006

top-soil layers, where the wetting and drying events occur more quickly, and reach maximum values at depths of 15–21 cm. The dynamics appear delayed when moving downward.

During rainfall events, the CO_2 concentration measurements may be subjected to errors, due to the amount of water that enters the macro-pores where the sensors are located. Under these circumstances, the estimates of CO_2 production, calculated as the difference between storage rate and vertical flux gradients (Eq. 7), are uncertain, as suggested by the abrupt reductions of S during rainfall events (Fig. 7). Similar problems have likely been encountered in other studies. For example, Chen et al. (2005) measured large positive increments in soil CO_2 concentrations during rainfall events (see Fig. 3 of Chen et al. (2005)), but only showed their estimates of soil CO_2 production during a particular soil dry-down (see Fig. 5 of Chen et al. (2005)). On the other hand, Jassal et al. (2005) did not report high rainfall-induced oscillations in CO_2 production probably because of their better estimate of the diffusivity. Also, in that study, the amount of precipitation per rain event was generally small and the soil well drained. These possible errors notwithstanding, the computed long-term rate in storage changes in this study remains negligible when compared to the flux divergence and CO_2 production. Jassal et al. (2005) reported a similar finding for a 54 years old Douglas-fir stand in Canada. Moreover, because the fluxes at depths below the root zone, z_R ($\sim$40–50 cm), are very small, the effluxes from the soil to the atmosphere, F_s, are close to the total S over the root depth, as can be seen by integrating Eq. 7 over depth, i.e.

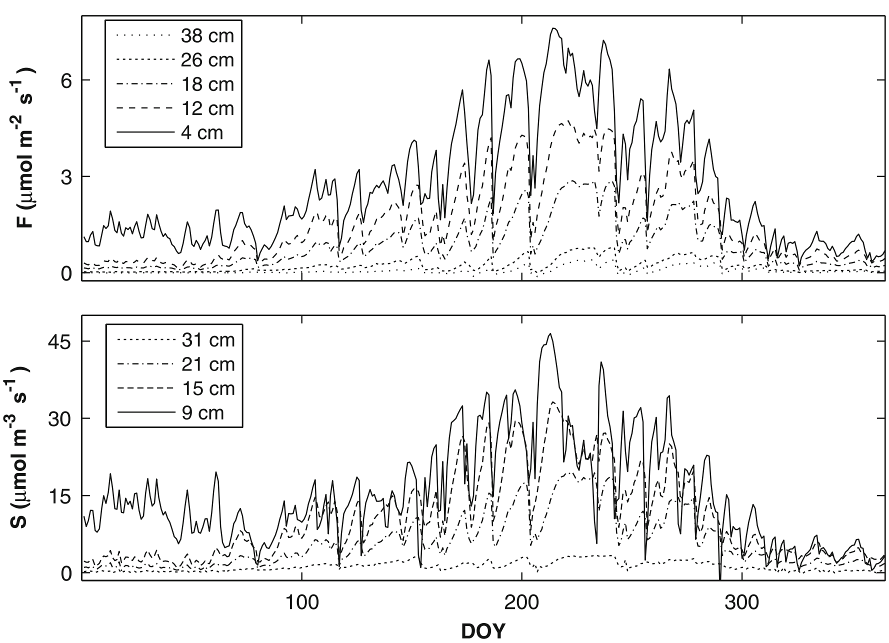

Fig. 7 Sample time series of estimated daily fluxes (*top*) and calculated daily production rates (*bottom*) at different depths in the plot AF1 (Table 1) during 2006

$$\int_{-z_R}^{0} \frac{dF}{dz} dz = F_s = \int_{-z_R}^{0} S dz. \quad (9)$$

Therefore, the measurement of the fluxes from the soil to the atmosphere can be considered roughly as an estimate of the CO_2 production within the root zone. Suwa et al. (2004) also estimated monthly CO_2 production over the entire 2 m soil column and found that the forest floor efflux is nearly balanced by the CO_2 production from the top 30 cm. We stress that the forest floor is in steady-state condition, and the balance between production and fluxes is commonly reached at time scales shorter than 30 min, as observed in Fig. 6. This is a major result when interpreting chamber measurements as an integrated measure of CO_2 production.

Vertical distribution and dynamics of CO_2 fluxes and production

The near-surface soil layer is the most active in terms of CO_2 production and fluxes, and both F and S rapidly decrease with increasing z (Fig. 7). The decrease in production with depth is consistent with the concomitant reduction in respiring root biomass (Matamala and Schlesinger 2000), while fluxes diminish because of the reduction of both production and soil diffusivity, the latter due to the higher water content. Decreasing flux with depth is the main reason CO_2 is higher in deeper layers.

Moreover, both F and S fluctuate temporally at two different timescales, daily and seasonal. Both follow daily cycles that mirror those of soil temperature (not shown), and exhibit strong seasonal cycles, especially at the surface, reaching maxima during the peak of the growing season in July and August. The seasonality of the fluxes is mainly due to the larger production during the growing season and to a high soil CO_2 diffusivity related to lower soil moisture levels, especially at the soil surface. The latter also explains why CO_2 concentrations close to the soil surface remain fairly stable during the growing season even though the production increases (Daly et al. 2008).

Figure 8 shows an example of the relationship between CO_2 production and θ and T_s. As expected, S decreases with depth because of the lower root density and high soil moisture. Relationships between

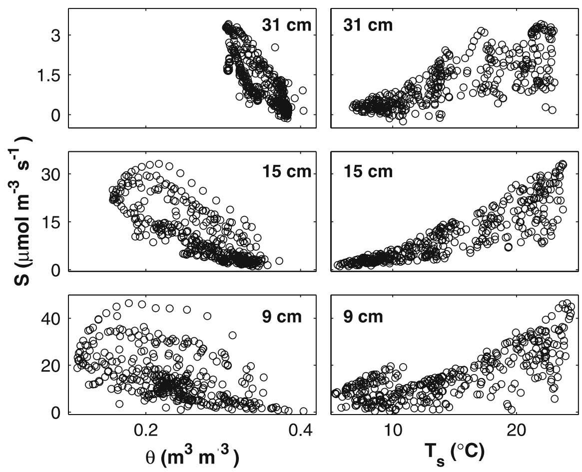

Fig. 8 Soil CO_2 production (S) as a function of local soil moisture (θ) and local soil temperature (T_s) at three different depths in the plot AF1 (Table 1) during the year 2006

production and both soil moisture and temperature can be identified. Higher temperatures ($T_s > 20°C$) lead to larger production, while low temperatures ($T_s < 12°C$) inhibit S. On the other hand, wetter conditions ($\theta > 0.26$) limit the production because they may generate an oxygen-limited environment, while when the soil is relatively dry ($\theta < 0.13$, which corresponds to relative soil moisture lower than 23%) the production is higher.

Limitations to comparisons between direct measurements and indirect estimates of CO_2 flux

The flux at the soil surface, F_s, calculated using Eqs. 5 and 6, can be used as an estimate for soil respiration, not including respiration occurring in the litter layer. It should be emphasized that this modeled F_s may be biased towards larger values because of the use of ambient atmospheric CO_2 concentration (enriched or control depending on the subplot) as a top boundary condition, when in fact, the CO_2 concentration just below the litter layer should be used. A comparison between daily fluxes estimated from Eqs. 5 to 6 and those measured with ACES, F_m, is shown in Fig. 9. At intermediate soil moisture in the upper 10 cm ($0.12 < \theta < 0.25$), a condition dominating the study period (see Juang et al. 2007, Fig. 1 for soil moisture histogram), modeled fluxes strongly correlate with the chamber-based estimates (Fig. 9a, b). Note that F_s only describes the efflux that would occur if the mineral soil were exposed to the atmosphere in ambient or enriched conditions. Conversely, F_m includes litter respiration. Thus, consistent with our finding, F_m is expected to exceed F_s, though F_s is likely to be over-estimated by this approach.

A sensitivity analysis on α (=10/3 in the formulation of tortuosity used in modeling diffusivity in Eq. 6) was also conducted. By reducing this parameter to 9/3, flux estimates from Eqs. 5 to 6 were always higher than the chamber measurements, while a similar increase in α set to $11/3 = 3.67$ resulted in estimated fluxes lower then the measurements by about 600–800 $g_C\ m^{-2}\ year^{-1}$. Because these differences are mainly related to the litterfall respiration, they cannot be much higher than 400 $g_C\ m^{-2}\ year^{-1}$ (Lichter et al. 2005; Palmroth et al. 2006). Hence, the value of $\alpha = 10/3$ appears reasonable for the site (consistent with the analysis in Suwa et al. 2004).

However, F_s tends to be higher than F_m in dry conditions, becoming lower than F_m in wet conditions (Fig. 9). Potential reasons for this discrepancy between modeled and measured efflux are numerous, but three plausible reasons can be readily identified: (1) the vertical resolution of sampling, (2) uncertainties in the parameters of the soil diffusivity (especially near the surface), and (3) the use of atmospheric CO_2 concentration rather than the use of the CO_2 concentration just beneath the litter. The

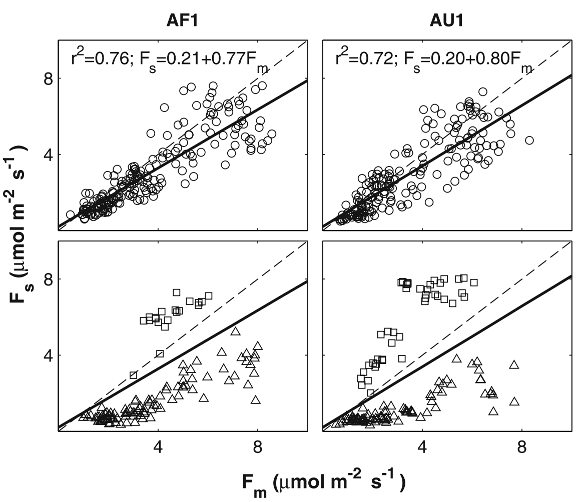

Fig. 9 Comparison between daily averages of chamber measured fluxes, F_m, and fluxes estimated from the CO_2 profiles, F_s, in the plots AF1 and AU1 (*top*). Wet ($\theta > 0.26$, *triangles*) and dry ($\theta < 0.13$, *squares*) conditions are shown separately (*bottom panels*). The intercepts of the regression lines are not significantly different from zero ($P > 0.1$)

selected sampling depths and the limitation of only one sensor at each depth reflect a compromise between cost of instruments, their volume averaging, and the objective to monitor the entire rooting depth. As a result, near-surface soil properties were not precisely known. These properties are probably influenced by macroporosity induced by the dense root system in the upper layers. Macroporosity affects the performance of Eqs. 5 to 6 differently for wet and dry soil moisture states. For wet soil moisture states, some of the CO_2 produced locally, especially at the surface, can escape horizontally and exit the soil system in localized air flushing events in the macropores adjacent to the large roots. A one-dimensional model cannot capture such lateral transport. Moreover, in wet conditions, the value of the diffusivity is likely to be underestimated by Eq. 6. Hence, the CO_2 efflux predicted by the model is smaller than the model prediction. In contrast, in dry conditions F_s tends to be higher than F_m. In fact, according to Eq. 6, dry conditions lead to diffusivity coefficients that solely depend on soil porosity ($D \sim n^{4/3}$). The estimate of diffusivity thus needs accurate information about n. This parameter is difficult to obtain, especially near the soil surface where the macroporosity is high and litterfall can have an important influence on diffusivity (Maier and Kress 2000). Moreover, according to the model of D of Eq. 6, soil with similar porosities, such as, e.g., sand and clay, are associated to same values of diffusivity in spite of their different textures. This is an unlikely situation, especially in a stratified soil such as that at the site (e.g., Thorbjørn et al. 2008).

Conclusions

High frequency subsurface soil CO_2 concentration and its relationship to soil water and temperature were analyzed in a temperate pine forest at two levels of atmospheric CO_2 concentration and soil nutrient availability during 2005 and 2006. Over these first 2 years, no significant treatment effect (enriched atmospheric CO_2, enriched soil N, or their interaction) was detected in either the values of C (averaged over the first 30 cm) or in F_s estimated from the C profiles.

Vertical profiles of C were found to be strongly affected by both temperature and soil water content.

At the hourly time scale, soil moisture and soil temperature interacted to determine daily *C* oscillations. At the daily and seasonal scales soil temperature appeared to control *C* at the deeper soil layers, while soil moisture was the main forcing near the surface, where *C* pulses can be primarily attributed to rainfall events. A linear relationship between the magnitude of *C* pulses and throughfall at the daily scale was observed for all the plots. Because these pulses appear independent of antecedent moisture conditions, they cannot be attributed to enhanced microbial activity, in as much as microbial activity is expected to be dependent on re-wetting cycles. The origin of these pulses can be attributed mainly to reductions in diffusivity following rainfall events.

In terms of fluxes and subsurface production, the forest was shown to be in a near steady-state condition (with very low changes in CO_2 storage). Such steady-state condition can be assumed to be reached at time scales shorter than 30 min. Both production and fluxes have a strong seasonal cycle. The larger CO_2 production during the growing season coupled to the higher CO_2 diffusivity, due to higher temperatures and lower soil moisture, generate rather stable CO_2 concentrations near the surface. Therefore, the modeling of CO_2 diffusivity plays a key role when evaluating CO_2 production and fluxes indirectly. The model of diffusivity becomes particularly important in wetter and drier than average conditions, as suggested by the comparison between direct measurements of soil efflux and the estimates obtained using the CO_2 concentration profiles. However, this finding needs to be further analyzed because the flux estimates from the profiles were calculated assuming values of CO_2 atmospheric concentrations that might be not reflective of the actual situation. However, we should note that atmospheric concentration is at least one order of magnitude smaller than soil CO_2 concentration; hence, quantities requiring the differencing between these two concentrations are always going to be dominated by the soil concentration, not the atmospheric.

Acknowledgments The authors would like to thank Judd Edeburn and the Duke Forest staff, and Keith Lewin and the Brookhaven National Laboratories staff, in particular Robert Nettles, for their assistance at the Duke Forest FACE site. E. D. thanks Luca Grossini for his help with some of the analyses. The authors also thank T. Christensen and an anonymous reviewer for their suggestions. This research was supported by the Office of Science (BER), U.S. Department of Energy, Grant no. DE-FG02-95ER62083.

References

Andrews JA, Schlesinger WH (2001) Soil CO_2 dynamics, acidification, and chemical weathering in a temperate forest with experimental CO_2 enrichment. Global Biogeochem Cycles 15:149–162. doi:10.1029/2000GB001278

Baldocchi D, Tang J, Xu L (2006) How switches and lags in biophysical regulators affect spatial-temporal variation of soil respiration in an oak-grass savanna. J Geophys Res 111:G02008. doi:10.1029/2005JG000063

Bernhardt ES, Barber JJ, Pippen JS, Taneva L, Andrews JA, Schlesinger WH (2006) Long-term effects of free air CO_2 enrichment (FACE) on soil respiration. Biogeochem 77:91–116. doi:10.1007/s10533-005-1062-0

Billings SA, Richter DD, Yarie J (1998) Soil carbon dioxide fluxes and profile concentrations in two boreal forests. Can J Res 28:1773–1783. doi:10.1139/cjfr-28-12-1773

Bowden RD, Davidson E, Savage K, Arabia C, Steudler P (2004) Chronic nitrogen additions reduce total soil respiration and microbial respiration in temperate forest soils at the Harvard Forest. For Ecol Manage 196:43–56. doi:10.1016/j.foreco.2004.03.011

Brady NC, Weil RR (2002) The nature and properties of soils. Prentice Hall, Upper Saddle River

Butnor JR, Johnsen KH (2004) Calibrating soil respiration measures with a dynamic flux apparatus using artificial soil media of varying porosity. Eur J Soil Sci 55:639–647. doi:10.1111/j.1365-2389.2004.00642.x

Butnor JR, Johnsen KH, Oren R, Katul G (2003) Reduction of forest floor respiration by fertilization on both carbon dioxide-enriched and reference 17-years-old loblolly pine stands. Glob Change Biol 9:849–861. doi:10.1046/j.1365-2486.2003.00630.x

Campbell GS, Norman JM (1998) An introduction to environmental biophysics, 2nd edn. Springer, New York

Cao M, Woodward FI (1998) Dynamic responses of terrestrial ecosystem carbon cycling to global climate change. Nature 393:249–252. doi:10.1038/30460

Chen D, Molina AE, Clapp CE, Venterea RT, Palazzo AJ (2005) Corn root influence on automated measurement of soil carbon dioxide concentrations. Soil Sci 170:779–787. doi:10.1097/01.ss.0000190512.41298.fc

Cox PM, Betts RA, Jones CD, Spall SA, Totterdel IJ (2000) Acceleration of global warming due to carbon-cycle feedbacks in a coupled climate model. Nature 408:184–187. doi:10.1038/35041539

Daly E, Oishi AC, Porporato A, Katul GG (2008) A stochastic model for daily subsurface CO_2 concentration and related soil respiration. Adv Water Resour 31:987–994. doi:10.1016/j.advwatres.2008.04.001

Davidson EA, Belk E, Boone R (1998) Soil water content and temperature as independent or confounded factors controlling soil respiration in a temperate mixed hardwood forest. Glob Change Biol 4:217–227. doi:10.1046/j.1365-2486.1998.00128.x

Davidson EA, Janssens IA, Luo Y (2006) On the variability of respiration in terrestrial ecosystems: moving beyond Q_{10}. Glob Change Biol 12:154–164. doi:10.1111/j.1365-2486.2005.01065.x

Fang C, Moncrieff JB (1999) A model for soil CO_2 production and transport. 1: model development. Agric For Meteorol 95:225–236. doi:10.1016/S0168-1923(99)00036-2

Finzi AC, Schlesinger WH (2002) Species control variation on litter decomposition in a pine forest exposed to elevated CO_2. Glob Change Biol 8:1217–1229. doi:10.1046/j.1365-2486.2002.00551.x

Finzi AC, Allen AS, DeLucia EH, Ellsworth DS, Schlesinger WH (2001) Forest litter production, chemistry, and decomposition following two years of free air CO_2 enrichment. Ecology 82:470–484

Flechard CR, Neftel A, Jocher M, Ammann C, Leifeld J, Fuhrer J (2007) Temporal changes in soil pore space CO_2 concentration and storage under permanent grassland. Agric For Meteorol 142:66–84. doi:10.1016/j.agrformet.2006.11.006

Freijer JI, Leffelaar PA (1996) Adapted Fick's law applied to soil respiration. Water Resour Res 32:791–800. doi:10.1029/95WR03820

Gaumont-Guay D, Black TA, Griffis TJ, Barr AG, Jassal RS, Nesic Z (2006) Interpreting the dependence of soil respiration on soil temperature and water content in a boreal aspen stand. Agric For Meteorol 140:220–235. doi:10.1016/j.agrformet.2006.08.003

Giardina CP, Ryan MG (2000) Evidence that decomposition rates of organic carbon in mineral soil do not vary with temperature. Nature 404:858–861. doi:10.1038/35009076

Glinski J, Stepniewski W (1985) Soil aeration and its role for plants. CRC Press, Boca Raton

Hashimoto S, Tanaka N, Kume T, Yoshifuji N, Hotta N, Tanaka K, Suzuki M (2007) Seasonality of vertically partitioned soil CO_2 production in temperate and tropical forest. J For Res 12:209–221. doi:10.1007/s10310-007-0009-9

Heath J, Ayres E, Possell M, Bardgett RD, Black HIJ, Grant H, Ineson P, Kerstiens G (2005) Rising atmospheric CO_2 reduces sequestration of root-derived soil carbon. Science 309:1711–1713. doi:10.1126/science.1110700

Hendrey G, Ellsworth D, Lewin K, Nagy J (1999) A free-air enrichment system for exposing tall forest vegetation to elevated atmospheric CO_2. Glob Change Biol 5:293–309. doi:10.1046/j.1365-2486.1999.00228.x

Hirano T, Kim H, Tanaka Y (2003) Long-term half-hourly measurement of soil CO_2 concentration and soil respiration in a temperate deciduous forest. J Geophys Res 108(D20):4631. doi:10.1029/2003JD003766

Hungate BA, Holland EA, Jackson RB, Chapin FSIII, Mooneyk HA, Field CB (1997) The fate of carbon in grassland under carbon dioxide enrichment. Nature 388:576–579. doi:10.1038/41550

Hyvonen R, Agren GI, Linder S et al (2007) The likely impact of elevated [CO_2], nitrogen deposition, increased temperature and management on carbon sequestration in temperate and boreal forest ecosystems: a literature review. New Phytol 173:463–480. doi:10.1111/j.1469-8137.2007.01967.x

Jassal RS, Black TA, Drewitt GB, Novak MD, Gaumont-Guay D, Nesic Z (2004) A model of the production and transport of CO_2 in soil: predicting soil CO_2 concentrations and CO_2 efflux from a forest floor. Agric For Meteorol 124:219–236. doi:10.1016/j.agrformet.2004.01.013

Jassal R, Black A, Novack M, Morgenstern K, Nesic Z, Gaumont-Guay D (2005) Relationship between soil CO_2 concentrations and forest-floor CO_2 effluxes. Agric For Meteorol 130:176–192. doi:10.1016/j.agrformet.2005.03.005

Juang J-Y, Porporato A, Stoy PC, Siqueira MBS, Oishi AC, Detto M, Kim HS, Katul GG (2007) Hydrologic and atmospheric controls on convective precipitation events in a southeastern US mosaic landscape. Water Resour Res W03421. doi:10.1029/2006WR004954

King JS, Hansonw PJ, Bernhardt E, Deangelis P, Norby RJ, Pregitzer KS (2004) A multiyear synthesis of soil respiration responses to elevated atmospheric CO_2 from four forest FACE experiments. Glob Change Biol 10:1027–1042. doi:10.1111/j.1529-8817.2003.00789.x

Lee X, Wu H-J, Sigler J, Oishi C, Siccama T (2004) Rapid and transient response of soil respiration to rain. Glob Change Biol 10:1017–1026

Lichter J, Barron S, Finzi A, Irving K, Roberts M, Stemmler E, Schlesinger WH (2005) Soil carbon sequestration and turnover in a pine forest after six years of atmospheric CO_2 enrichment. Ecology 86:1835–1847. doi:10.1890/04-1205

Maier CA, Kress LW (2000) Soil CO_2 evolution and root respiration in 11 year-old loblolly pine (*Pinus taeda*) plantations as affected by moisture and nutrient availability. Can J For Res 30:347–359. doi:10.1139/cjfr-30-3-347

Makipaa R (1995) Effect of nitrogen input on carbon accumulation of boreal forest soils and ground vegetation. For Ecol Manage 79:217–226. doi:10.1016/0378-1127(95)03601-6

Matamala R, Schlesinger WH (2000) Effects of elevated atmospheric CO_2 on fine root production and activity in an intact temperate forest ecosystem. Glob Change Biol 6:967–979. doi:10.1046/j.1365-2486.2000.00374.x

Millington RJ (1959) Gas diffusion in porous media. Science 130:100–102. doi:10.1126/science.130.3367.100-a

Millington RJ, Quirk JM (1961) Permeability of porous solids. Trans Faraday Soc 57:1200–1207. doi:10.1039/tf9615701200

Oh NH, Richter DD (2005) Elemental translocation and loss from three highly weathered soil–bedrock profiles in the southeastern United States. Geoderma 126:5–25. doi:10.1016/j.geoderma.2004.11.005

Olsson P, Linder S, Giesler R, Hogberg P (2005) Fertilization of boreal forest reduces both autotrophic and heterothropic soil respiration. Glob Change Biol 11:1745–1753. doi:10.1111/j.1365-2486.2005.001033.x

Oren R, Pataki DE (2001) Transpiration in response to variation in microclimate and soil moisture in southeastern deciduous forests. Oecologia 127:549–559. doi:10.1007/s004420000622

Oren R, Ewers BE, Todd P, Phillips N, Katul G (1998) Water balance delineates the soil layer in which moisture affects canopy conductance. Ecol Appl 8:990–1002. doi:10.1890/1051-0761(1998)008[0990:WBDTSL]2.0.CO;2

Oren R, Ellsworth DS, Johnsen KH, Phillips N, Ewers BE, Maier C, Schafer KVR, McCarthy H, Hendrey G, McNulty SG, Katul GG (2001) Soil fertility limits carbon sequestration by forest ecosystems in a CO_2-enriched atmosphere. Nature 411:469–472. doi:10.1038/35078064

Oren R, Hsieh C-I, Stoy P, Albertson J, McCarthy HR, Harrell P, Katul GG (2006) Estimating the uncertainty in annual net ecosystem carbon exchange: spatial variation in turbulent fluxes and sampling errors in eddy-covariance measurements. Glob Change Biol 12:883–896. doi:10.1111/j.1365-2486.2006.01131.x

Palmroth S, Maier CA, McCarthy HR, Oishi AC, Kim H-S, Johnsen KH, Katul GG, Oren R (2005) Contrasting responses to drought of forest floor CO_2 efflux in a Loblolly pine plantation and a nearby Oak-Hickory forest. Glob Change Biol 11:1–14. doi:10.1111/j.1365-2486.2005.00915.x

Palmroth S, Oren R, McCarthy HR, Johnsen KH, Finzi AC, Butnor JR, Ryan MG, Schlesinger WH (2006) Above-ground sink strength in forests controls the allocation of carbon below ground and its CO_2-induced enhancement. Proc Natl Acad Sci USA 103:19362–19367. doi:10.1073/pnas.0609492103

Patwardhan AS, Nieber JL, Moore ID (1988) Oxygen, carbon dioxide, and water transfer in soils: mechanisms and crop response. Trans Am Soc Agr Eng 31:1383–1395

Phillips RP, Fahey TJ (2007) Fertilization effects on fineroot biomass, rhizosphere microbes and respiratory fluxes in hardwood forest soils. New Phytol 176:655–664. doi:10.1111/j.1469-8137.2007.02204.x

Phillips N, Oren R (2001) Intra- and inter-annual variation in transpiration of a pine forest. Ecol Appl 11:385–396. doi:10.1890/1051-0761(2001)011[0385:IAIAVI]2.0.CO;2

Pumpanen J, Ilvesniemi H, Hari P (2003) A process-based model for predicting soil carbon dioxide efflux and concentration. Soil Sci Soc Am J 67:402–413

Raich JW, Schlesinger WH (1992) The global carbon dioxide flux in soil respiration and its relationship to vegetation and climate. Tellus 44B:81–99

Rustad LE, Fernandez IJ (1998) Experimental soil warming effects on CO_2 and CH_4 flux from a low elevation spruce-fir forest soil in Maine, USA. Glob Change Biol 4:597–605. doi:10.1046/j.1365-2486.1998.00169.x

Savitzky A, Golay MJE (1964) Smoothing and differentiation of data by simplified least squares procedures. Anal Chem 36:1627–1639. doi:10.1021/ac60214a047

Schäfer KV, Oren R, Lai CT, Katul GG (2002) Hydrologic balance in an intact temperate forest ecosystem under ambient and elevated atmospheric CO_2 concentration. Glob Change Biol 8:895–911

Schimel DS (1995) Terrestrial ecosystems and the carbon cycle. Glob Change Biol 1:77–91. doi:10.1111/j.1365-2486.1995.tb00008.x

Schlesinger WH (1997) Biogeochemistry: an analysis of global change. Academy Press, San Diego

Simunek J, Suarez DL (1993) Modeling of carbon dioxide transport and production in soil. I. Model development. Water Resour Res 29:487–497. doi:10.1029/92WR02225

Steel GD, Torrie JH, Dickey DA (1997) Principles and procedures of statistics: a biometrical approach, 3rd edn. McGraw-Hill, New York

Suwa M, Katul GG, Oren R, Andrews J, Pippen J, Mace A, Schlesinger WH (2004) Impact of elevated atmospheric CO_2 on forest floor respiration in a temperate pine forest. Global Biogeochem Cycles 18:GB2013. doi:10.129/2003GB002182

Takle ES, Massman WJ, Brandle JR et al (2004) Influence of high-frequency ambient pressure pumping on carbon dioxide efflux from soil. Agric For Meteorol 124:193–206. doi:10.1016/j.agrformet.2004.01.014

Taneva L, Pippen JS, Schlesinger WH, Gonzalez-Meler MA (2006) The turnover of carbon pools contributing to soil CO_2 and soil respiration in a temperate forest exposed to elevated CO_2 concentration. Glob Change Biol 12:983–994. doi:10.1111/j.1365-2486.2006.01147.x

Tang J, Baldocchi DD, Qi Y, Xu L (2003) Assessing soil CO_2 efflux using continuous measurements of CO_2 profiles in soils with small solid-state sensors. Agric For Meteorol 124:193–206

Thorbjørn A, Moldrup P, Blendstrup H, Komatsu T, Rolston DE (2008) A gas diffusivity model based on air-, solid-, and water-phase resistance in variably saturated soil. Vadose Zone J 7:1276–1286. doi:10.2136/vzj2008.0023

Thorstenson DC, Pollock DW (1989) Gas transport in unsaturated zones: multicomponent systems and the adequacy of Fick's laws. Water Resour Res 25:477–507. doi:10.1029/WR025i003p00477

Trumbore SE, Chadwick OA, Amundson R (1996) Rapid exchange between soil carbon and atmospheric carbon dioxide driven by temperature change. Science 272:393–396. doi:10.1126/science.272.5260.393

Winston GC, Sundquist ET, Stephens BB, Trumbore SE (1997) Winter CO_2 fluxes in a boreal forest. J Geophys Res 102(D24):28795–28804. doi:10.1029/97JD01115

Xu L, Baldocchi DD, Tang J (2004) How soil moisture, rain pulses, and growth alter the response of ecosystem respiration to temperature. Global Biogeochem Cycles 18:GB4002. doi:10.1029/2004GB002281

Zak DR, Pregitzer KS, King JS, Holmes WE (2000) Elevated atmospheric CO_2, fine roots and the response of soil microorganisms: a review and hypothesis. New Phytol 147:201–222. doi:10.1046/j.1469-8137.2000.00687.x